LHCb-PUB-2009-031
January 13, 2010

Invariant mass line shape of $B \to PP$ decays at LHCb

A. Carbone[1], D. Galli[1], U. Marconi[1], S. Perazzini[1], A. Sarti[2],
V. Vagnoni[1], G. Valenti[1].

[1] *Istituto Nazionale di Fisica Nucleare, Sezione di Bologna, Italy*
[2] *Istituto Nazionale di Fisica Nucleare, Laboratori Nazionali di Frascati, Italy*

Abstract

The family of B meson decays into pairs of charmless charged pseudo-scalar mesons comprises many different channels. In order to disentagle the overlapping mass peaks of the various decay modes, an accurate description of the invariant mass distribution of each mode is required. In particular, the invariant mass parameterization must take into account the effect of QED final state radiation, which leads to the presence of a long tail on the lower side of the mass peak. In this document we propose a new parameterization based on a complete QED calculation of the photon emission rate and we compare it to a simpler one based on phenomenological arguments. Furthermore, we show how the shape of the invariant mass distributions under the $\pi^+\pi^-$ mass hypothesis, for every decay mode of interest, can be described very precisely by means of analytical calculations.

1 Introduction

The LHCb detector [1] can reconstruct some 10^5 $H_b \to h^+h'^-$ events per year which can be exploited for $\mathcal{CP}$ violation measurements [2]. These unprecedented sample sizes are a consequence of the large beauty production cross section at the LHC, which is expected to be around 500 μb [3], and of the design of the detector, specifically optimized for performing B-physics measurements.

Due to the simultaneous production of B^0, B_s^0 and Λ_b hadrons, the mass peaks of many two-body decays overlap, giving rise to a single unresolved signal, if no particle identification information is used. Excellent control of the particle identification observables and an event-by-event fit technique are then required to fully exploit the statistical power of the sample. An accurate description of the invariant mass distribution of each $H_b \to h^+h'^-$ decay mode is a key ingredient for such an event-by-event fit.

The parameterization of the invariant mass spectrum is complicated by the fact that the decay products radiate final state photons, hence leading to a distortion of the shape of the charged pair invariant mass. The net effect, as we shall see, is the presence of a long tail on the lower side of the mass peak.

In Sec. 3 we will show how the knowledge of the theoretical decay rate including QED radiation, briefly discussed in Sec. 2, can be succesfully employed for describing the reconstructed invariant mass line shape of these decays. Another important aspect for realizing a simultaneous fit with all the decay modes included [2] is the description of the invariant mass line shape under a common mass hypothesis, that we conventionally choose as the $\pi^+\pi^-$ one. We will discuss in Sec. 4 how such a description can be achieved by means of analytical calculations.

2 Theoretical aspects of QED final state radiation

The LHCb Monte Carlo (MC) simulation includes final state radiation by means of the PHOTOS generator [4], that is run on top of the EvtGen decay generator [5] and adds radiated photons to the decay tree.

PHOTOS is a MC algorithm that simulates QED photon emissions in decays, by calculating $\mathcal{O}(\alpha)$ radiative corrections for charged particles using a leading log collinear approximation. Within this approximation, the program calculates the amount of bremsstrahlung radiation in the decay and modifies the final state according to the decay topology. A simplified algorithm like PHOTOS is commonly used since calculating more complete radiative corrections in heavy meson decays pose difficult theoretical problems, due to the lack of a universally valid effective theory. However, it is possible to calculate and parameterize infra-red effects using the approximation of point-like hadrons. An important step in this direction can be found in Ref. [6], where the calculation has been performed for the non-leptonic decays of B and D mesons to two pseudo-scalar mesons. Ref. [6] reports a complete $\mathcal{O}(\alpha)$ calculation, which takes into account infra-red effects due to virtual and real photons. According to the results of this calculation, the differential decay rate to

$\mathcal{O}(\alpha)$ of a $B \to hh + n\gamma$ decay, where n stands for any number of emitted photons, can be written as:

$$\frac{d\Gamma_{12}^{incl}}{dE} = \frac{2\alpha}{\pi}\frac{|b_{12}|\Gamma_{12}^{0}}{E}\left(\frac{2E}{m_B}\right)^{\frac{2\alpha}{\pi}|b_{12}|} \tag{1}$$

where E is the sum of the energies of the emitted photons in the rest frame of the decaying B meson, Γ_{12}^{0} represents the pure weak decay rate (that is *de facto* unobservable) and m_B is the mass of the decaying B meson. The term b_{12} is given by:

$$b_{12} = 1 - \frac{4 - \Delta_1^2 - \Delta_2^2 + 2\delta^2}{8\delta}\log\left(\frac{\Delta_1 + \delta}{\Delta_1 - \delta}\cdot\frac{\Delta_2 + \delta}{\Delta_2 - \delta}\right), \tag{2}$$

with

$$\Delta_{1(2)} = 1 + r_{1(2)}^2 - r_{2(1)}^2 \qquad r_i = \frac{m_i}{m_B} \tag{3}$$

and

$$\delta = \sqrt{[1 - (r_1 + r_2)^2]\,[1 - (r_1 - r_2)^2]}, \tag{4}$$

where m_1 and m_2 are the masses of the two pseudo-scalar mesons.

Considering for simplicity the case of a single photon emission (multiple emissions are suppressed by the corresponding powers of α), m_B is given by:

$$m_B = E_1 + E_2 + E_\gamma, \tag{5}$$

where E_1, E_2 and E_γ are the energies of the two pseudo-scalars and of the photon in the rest frame of the B, where by definition we have:

$$\vec{p}_1 + \vec{p}_2 + \vec{p}_\gamma = 0. \tag{6}$$

The invariant mass of the two pseudo-scalars alone m_{12} is then given by:

$$m_{12}^2 = (E_1 + E_2)^2 - (\vec{p}_1 + \vec{p}_2)^2 = (E_1 + E_2)^2 - E_\gamma^2, \tag{7}$$

and then we can conclude that

$$m_{12} = m_B\sqrt{1 - \frac{2E_\gamma}{m_B}} \simeq m_B - E_\gamma. \tag{8}$$

In other words, the effect of the missing photon is a leakage in the measured invariant mass equal to the photon energy in the rest frame of the B.

3 Parameterization under the correct mass hypothesis

Since the expression of the photon energy is given by Eq. (1), we can write the p.d.f. for the invariant mass of the two charged daughters, ignoring for the moment experimental effects, as:

$$f(m) = \Theta(m_B - m)\frac{s+1}{(m_B - m_{min})^{s+1}}(m_B - m)^s, \tag{9}$$

where $\Theta(m_B - m)$ is the Heaviside function, $m_{min} = 5\,\mathrm{GeV/c^2}$ is the lower limit of the invariant mass accepted by the offline event selection, and the parameter s is given by:

$$s = \frac{2\alpha}{\pi}|b_{12}| - 1. \tag{10}$$

Since s is numerically less than zero (in fact it is close to -1), $f(m)$ diverges for $m \to m_B$. Nevertheless, the p.d.f. is integrable and correctly normalized to one.

In order to take into account the experimental resolution, $f(m)$ can be convoluted with the sum of two Gaussian p.d.f.'s:

$$g(m) = \Theta(m_B - m')\, A\, (m_B - m')^s \otimes G_d(m - m';\, f_1,\, \sigma_1,\, \sigma_2) \tag{11}$$

where A is a normalization factor, and with G_d defined as:

$$G_d(m - \mu;\, f_1,\, \sigma_1,\, \sigma_2) = \frac{f_1}{\sqrt{2\pi}\sigma_1} e^{-\frac{(m-\mu)^2}{2\sigma_1^2}} + \frac{1 - f_1}{\sqrt{2\pi}\sigma_2} e^{-\frac{(m-\mu)^2}{2\sigma_2^2}}. \tag{12}$$

The convolution in Eq. (11) cannot be calculated analytically, hence it must be calculated numerically. Unfortunately, due to both the fast rise and divergence of $f(m)$ for $m \to m_B$, such numerical computation is not straightforward, either using a Fast Fourier Transform technique or a numerical integration. In order to overcome numerical problems, $f(m)$ has been approximated as follows:

$$f(m) = w\Theta(m_B - m - \epsilon)\frac{s+1}{(m_B - m_{min})^{s+1} - \epsilon^{s+1}}\,(m_B - m)^s + (1 - w)\,\delta(m_B - m) \tag{13}$$

where ϵ represents a small cutoff that determines the splitting of $f(m)$ in two parts, a regular one plus a Dirac δ function. The weight w is given by:

$$w = 1 - \left(\frac{\epsilon}{m_B - m_{min}}\right)^{s+1}. \tag{14}$$

We can now rewrite $g(m)$ as in the following:

$$\begin{aligned} g(m) &= w\Theta(m_B - m' - \epsilon)\, A'\, (m_B - m')^s \otimes G_d(m - m';\, f_1,\, \sigma_1,\, \sigma_2) + \\ &+ (1 - w)\, B'\, G_d(m - m_B;\, f_1,\, \sigma_1,\, \sigma_2) \end{aligned} \tag{15}$$

where A' and B' are two normalization factors, and where the remaining convolution no longer presents numerical problems since the function is regular and finite in the entire domain. The choice of ϵ is somewhat arbitrary; it should be small enough in order to properly take into account softer photons, but not too small as again to lead to numerical troubles. For our practical purposes, we find that setting $\epsilon = 10\,\mathrm{keV/c^2}$ satisfies both the requirements.

Before performing fits to the invariant mass distributions, we need to introduce a further ingredient. Eq. (15) assumes that the selection efficiency (the offline and online

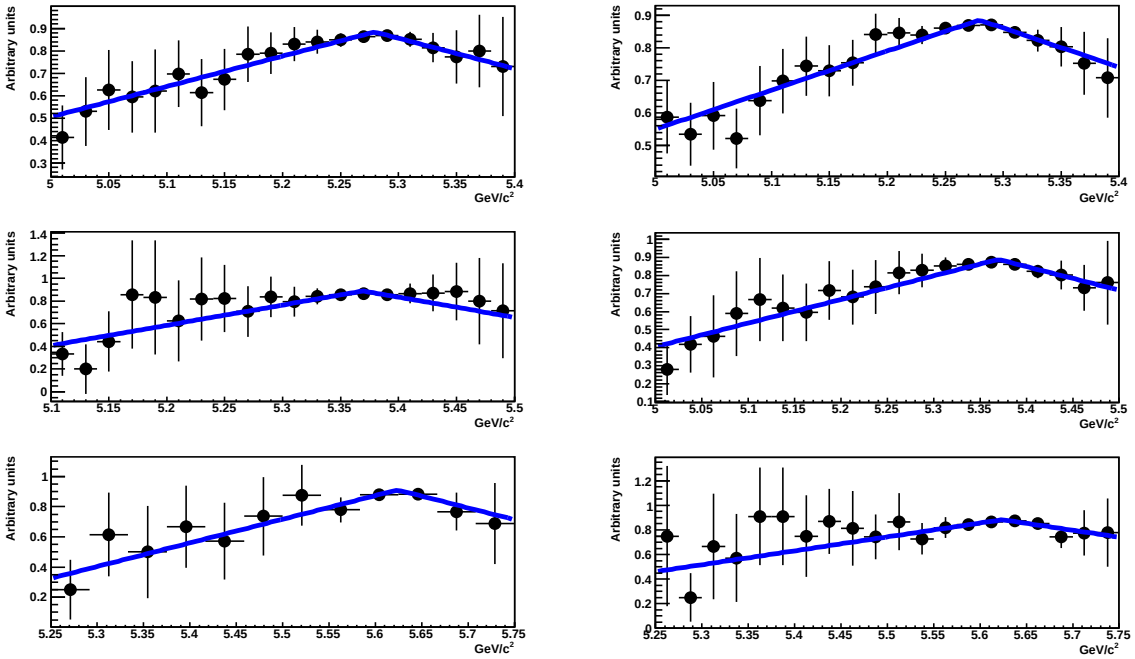

Figure 1: Relative dependence on the invariant mass of the event selection acceptance, with superimposed a χ^2 fit of Eq. (16): $B^0 \to \pi^+\pi^-$ (top left), $B^0 \to K^+\pi^-$ (top right), $B_s^0 \to \pi^+K^-$ (middle left), $B_s^0 \to K^+K^-$ (middle right), $\Lambda_b \to p\pi^-$ (bottom left) and $\Lambda_b \to pK^-$ (bottom right).

event selections are described in Ref. [2]) has no dependence on the invariant mass value. As is clear from Fig. 1, however, the efficiency has an appreciable dependence on the mass. This dependence can be approximated by a linear relation within the mass window:

$$\epsilon_m(m) \propto 1 + q \cdot |m - m_B|, \tag{16}$$

where q is a free parameter to be determined. The main cause of this mass dependence introduced by the event selection is the cut on the impact parameter of the B hadron with respect to the primary vertex. This cut is used to constrain the B hadron momentum to point to the primary vertex, but in case of missing (or excessive) momentum of the charged daughters, the reconstructed B momentum pointing to the primary vertex is altered. Consequently, this cut introduces a dependence of the selection efficiency on the B invariant mass value, which is visible in Fig. 1. The values of the q parameters resulting from the fits are summarized in Tab. 1. There is no evidence for any dependence of the results on the decay channel. The average value of the q parameter is $q = (-1.5 \pm 0.1)\,\mathrm{c}^2/\mathrm{GeV}$.

By multiplying $g(m)$ of Eq. (15) by this acceptance, we finally get a p.d.f. for m:

$$h(m) = K^{-1}\, g(m) \cdot (1 + q \cdot |m - m_B|), \tag{17}$$

Channel	q [c^2/GeV]
$B^0 \to \pi^+\pi^-$	-1.5 ± 0.3
$B^0 \to K^+\pi^-$	-1.4 ± 0.2
$B^0_s \to \pi^+K^-$	-2.0 ± 0.5
$B^0_s \to K^+K^-$	-1.5 ± 0.2
$\Lambda_b \to p\pi^-$	-1.7 ± 0.4
$\Lambda_b \to pK^-$	-1.3 ± 0.4
Average	-1.5 ± 0.1

Table 1: Results of the fits to the invariant mass dependence of the selection efficiency, using Eq. (16).

Channel	μ [MeV/c^2]	f_G	σ_1 [MeV/c^2]	σ_2 [MeV/c^2]	s	μ_{MC} [MeV/c^2]	s_{th}
$B^0 \to \pi^+\pi^-$	5279.1 ± 0.2	0.83 ± 0.02	18.9 ± 0.3	49 ± 2	-0.971 ± 0.002	5279.4	-0.971
$B^0 \to K^+\pi^-$	5279.1 ± 0.1	0.83 ± 0.01	18.6 ± 0.2	47 ± 1	-0.977 ± 0.001	5279.4	-0.977
$B^0_s \to \pi^+K^-$	5369.2 ± 0.5	0.88 ± 0.02	19.2 ± 0.5	57 ± 3	-0.984 ± 0.003	5369.6	-0.977
$B^0_s \to K^+K^-$	5368.9 ± 0.2	0.84 ± 0.02	19.2 ± 0.3	47 ± 2	-0.984 ± 0.001	5369.6	-0.983
$\Lambda_b \to p\pi^-$	5623.9 ± 0.7	0.90 ± 0.03	19.3 ± 0.6	57 ± 7	-0.981 ± 0.004	5624.0	-0.979
$\Lambda_b \to pK^-$	5624.3 ± 0.5	0.84 ± 0.04	18.9 ± 0.7	49 ± 4	-0.984 ± 0.003	5624.0	-0.985

Table 2: Results of the fits to the invariant mass distributions of the p.d.f. defined by Eq. (17). For comparison, the last two columns show the B mass values used in the MC simulation and the theoretical expectation for the parameter s respectively.

where the normalization factor K is given by:

$$K = \int_{m_{min}}^{m_{max}} g(m') \cdot (1 + q \cdot |m' - m_B|) dm'. \tag{18}$$

Fig. 2 shows the invariant mass distributions of all the channels under study with the result of an unbinned likelihood fit using the p.d.f. defined by Eq. (17). The numerical results of the fits are shown in Tab. 2.

The fitted values of the s parameters are notably compatible with the theoretical expectations s_{th}, calculated using Eq. (10). However, the fits seem to indicate that a small systematic shift downwards of the B mass values by about 300 keV/c^2 still remains, and its proper understanding deserves further study. Note that the formalism outlined above just applies to decays of B mesons to two pseudo-scalars, hence it is not strictly valid for the two Λ_b decays. Nonetheless, we have used the same p.d.f. in the fits to the two Λ_b modes. It can be seen that indeed the p.d.f. fits very well to the two Λ_b invariant mass distributions, with results which are consistent to those of the B meson fits.

Although the parameterization discussed above is well motivated on theoretical grounds and the fits give good results, its usage is not in general practical when performing high statistics toy MC studies of the sensitivity on $\mathcal{CP}$ violating observables, discussed in Ref [2], since the time needed for the numerical computation of the convolution would dominate the calculation of the likelihood function. In this case, instead of

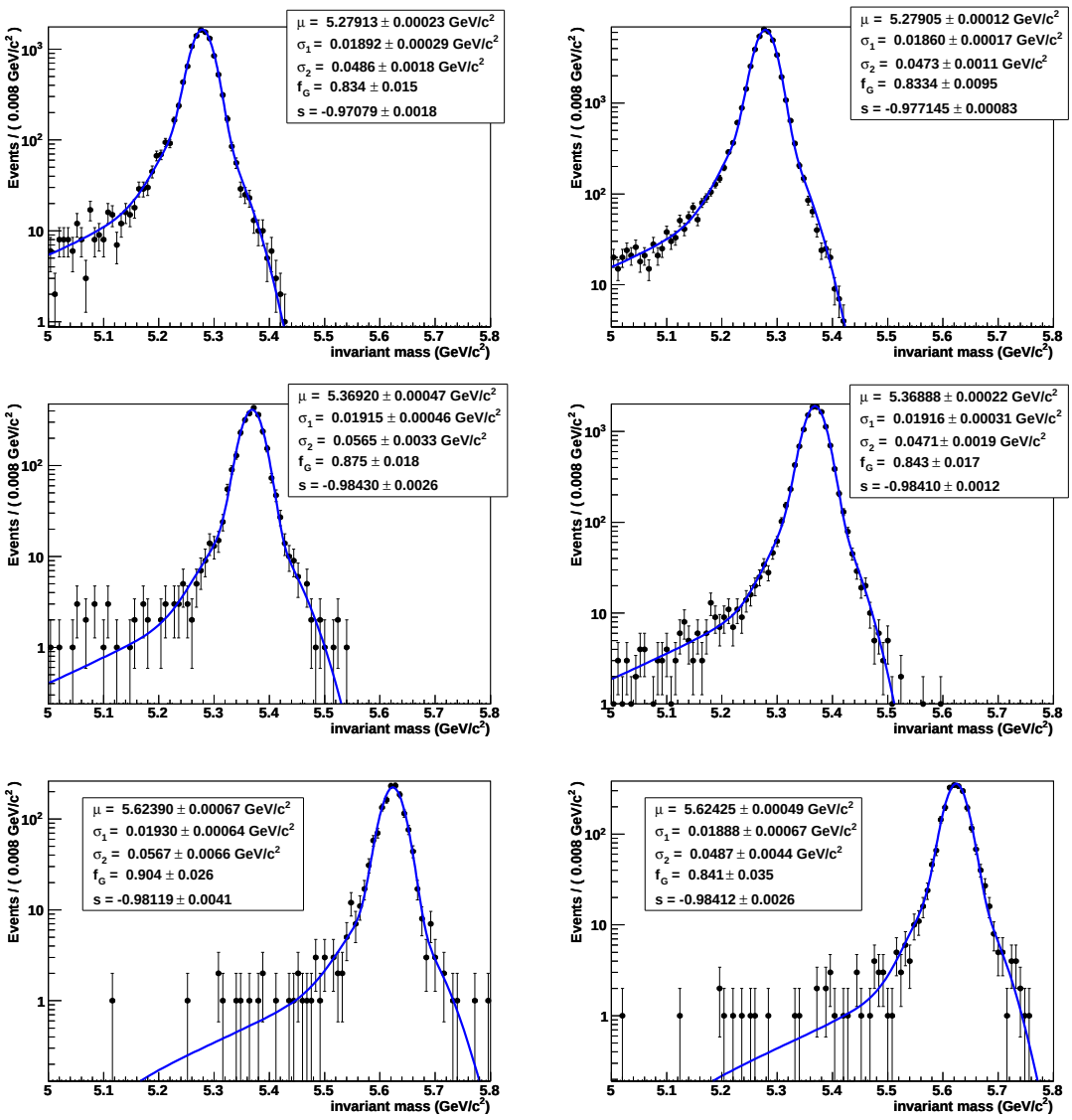

Figure 2: Invariant mass distributions of the various modes, with superimposed the result of the fit of the p.d.f. defined by Eq. (17): $B^0 \to \pi^+\pi^-$ (top left), $B^0 \to K^+\pi^-$ (top right), $B_s^0 \to \pi^+K^-$ (middle left), $B_s^0 \to K^+K^-$ (middle right), $\Lambda_b \to p\pi^-$ (bottom left) and $\Lambda_b \to pK^-$ (bottom right).

using the expression given in Eq. (13) for $f(m)$, we write:

$$f(m) = f_E\,\Theta(m_B - m)\,\frac{1}{r}e^{-r(m_B-m)} + (1 - f_E)\,\delta(m_B - m), \tag{19}$$

i.e. we decompose the mass distribution, in the absence of detector effects, into an exponential p.d.f. describing events where the emission of photons took place, plus a component with no emission. The factor f_E weights the number of events where radiation

Channel	μ [MeV/c^2]	f_G	σ_1 [MeV/c^2]	σ_2 [MeV/c^2]	f_E	r [c^2/GeV]	μ_{MC} [MeV/c^2]
$B^0 \to \pi^+\pi^-$	5278.5 ± 0.3	0.832 ± 0.018	18.8 ± 0.3	47 ± 2	0.066 ± 0.007	9.6 ± 1.2	5279.4
$B^0 \to K^+\pi^-$	5278.5 ± 0.1	0.835 ± 0.010	18.5 ± 0.2	46 ± 1	0.049 ± 0.003	9.1 ± 0.7	5279.4
$B_s^0 \to \pi^+K^-$	5368.5 ± 0.5	0.86 ± 0.02	18.9 ± 0.5	54 ± 4	0.024 ± 0.007	3.6 ± 2.6	5369.6
$B_s^0 \to K^+K^-$	5368.4 ± 0.2	0.838 ± 0.017	18.9 ± 0.3	45 ± 2	0.035 ± 0.004	8.4 ± 1.1	5369.6
$\Lambda_b \to p\pi^-$	5623.5 ± 0.6	0.90 ± 0.03	19.1 ± 0.7	53 ± 7	0.053 ± 0.014	9.9 ± 2.0	5624.0
$\Lambda_b \to pK^-$	5623.7 ± 0.5	0.83 ± 0.03	18.7 ± 0.7	47 ± 4	0.029 ± 0.006	5.7 ± 1.3	5624.0

Table 3: Results of the fits to the invariant mass distributions of the p.d.f. defined by Eq. (20). For comparison, the last column shows the mass value used in the MC simulation. The average width defined as $\sigma = \sqrt{f_1\sigma_1^2 + (1-f_1)\sigma_2^2}$ is about 25 MeV/c^2.

occurred with respect to events with no radiation. In practice, we replace the hyperbolically divergent behaviour of the mass distribution for $m \to m_B$ with a regular exponential, which is of course finite for $m = m_B$. From a physical point of view, such approximation corresponds to an underestimation of the rate of soft photon emissions of low energies. Taking into account resolution effects, the p.d.f. $g(m)$ becomes:

$$g(m) = f_E\, E_d(m - m_B;\, f_1,\, \sigma_1,\, \sigma_2,\, r) + (1 - f_E)\, C\, G_d(m - m_B;\, f_1,\, \sigma_1,\, \sigma_2), \qquad (20)$$

where C is a normalization factor, and E_d is defined as:

$$\begin{aligned} E_d(m - m_B;\, f_1,\, \sigma_1,\, \sigma_2,\, r) \;&=\; f_1\, K_1^{-1} e^{r(m-m_B)} \left[1 - \mathrm{Erf}\left(\frac{m - m_B + r\sigma_1^2}{\sqrt{2}\sigma_1}\right)\right] + \qquad (21) \\ &+\; (1 - f_1)\, K_2^{-1} e^{r(m-m_B)} \left[1 - \mathrm{Erf}\left(\frac{m - m_B + r\sigma_2^2}{\sqrt{2}\sigma_2}\right)\right]. \end{aligned}$$

The normalization factors $K_{1(2)}$ are given by:

$$K_{1(2)} = \int_{m_{min}}^{m_{max}} e^{r(m-m_B)} \left[1 - \mathrm{Erf}\left(\frac{m - m_B + r\sigma_{1(2)}^2}{\sqrt{2}\sigma_{1(2)}}\right)\right] dm, \qquad (22)$$

with $m_{min} = 5\,\mathrm{GeV/c^2}$ and $m_{max} = 5.8\,\mathrm{GeV/c^2}$, corresponding to the mass window accepted by the offline selection. The integral in Eq. (22) can be calculated analytically, hence the whole expression of the $g(m)$ p.d.f. is analytic and no longer involves lengthy numerical computations.

Fig. 3 shows the invariant mass distributions of each decay mode with the result of an unbinned likelihood fit using the p.d.f. defined by Eq. (20). The numerical results of the fits are shown in Tab. 3.

The bias of the mass values of the B hadrons are much larger than before, exceeding in most cases 1 MeV/c^2. This is expected since, as stated previously, this parameterization clearly underestimates the emission of low energy photons. Note that we are ignoring any dependence of the selection efficiency on the invariant mass value in this case, as using such a phenomenological parameterization an efficiency correction would not lead to any practical improvement of knowledge. As far as the fractions and the widths of the Gaussian p.d.f.'s are concerned, they are practically equal to those obtained previously and shown in Tab. 2.

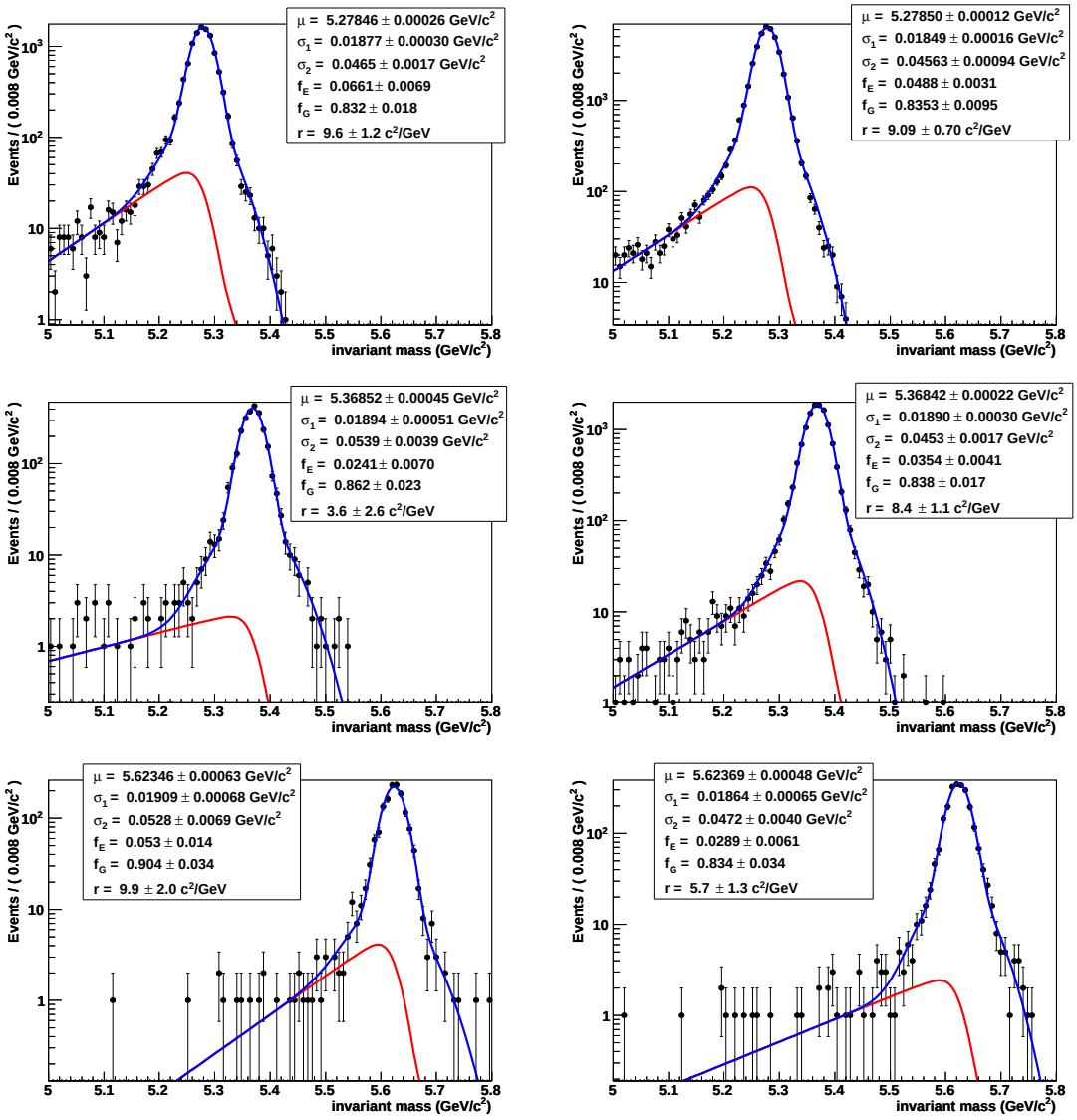

Figure 3: Invariant mass distributions of the various modes, with superimposed the result of the fit of the p.d.f. defined by Eq. (20): $B^0 \to \pi^+\pi^-$ (top left), $B^0 \to K^+\pi^-$ (top right), $B_s^0 \to \pi^+K^-$ (middle left), $B_s^0 \to K^+K^-$ (middle right), $\Lambda_b \to p\pi^-$ (bottom left) and $\Lambda_b \to pK^-$ (bottom right). As a reference, the lighter curve represents just the first component of Eq. (20), i.e. the one representing the radiation tail.

4 Parameterization under the $\pi^+\pi^-$ hypothesis

All studies presented hitherto assume the correct mass hypotheses for the daughter particles. In this section we will show how to parameterize the invariant mass if instead one ignores any information on the masses of the daughter particles, in particular making the

conventional assumption that the daughter particles are pions for every decay mode.

For a generic $H_b \to h^+h'^-$ decay, the B mass squared is given by:

$$m_B^2 = m_{h^+}^2 + m_{h'^-}^2 + 2\sqrt{p_+^2 + m_{h^+}^2}\sqrt{p_-^2 + m_{h'^-}^2} - 2\vec{p}_+ \cdot \vec{p}_-, \tag{23}$$

where m_{h^+} and m_{h^-} are the masses of the positive and negative decay products, and p_+ and p_- their momenta. If we make the $\pi^+\pi^-$ hypothesis for the final state particles, we can write:

$$m_{\pi\pi}^2 = m_\pi^2 + m_\pi^2 + 2\sqrt{p_+^2 + m_\pi^2}\sqrt{p_-^2 + m_\pi^2} - 2\vec{p}_+ \cdot \vec{p}_-. \tag{24}$$

By subtracting these two equations we obtain:

$$\begin{aligned} m_B^2 - m_{\pi\pi}^2 &= (m_{h^+}^2 - m_\pi^2) + (m_{h^-}^2 - m_\pi^2) + \\ &+ 2 \cdot \left(\sqrt{p_+^2 + m_{h^+}^2}\sqrt{p_-^2 + m_{h'^-}^2} - \sqrt{p_+^2 + m_\pi^2}\sqrt{p_-^2 + m_\pi^2} \right). \end{aligned} \tag{25}$$

In the limit of small particle masses with respect to the momenta, the previous identity can be approximated as:

$$\begin{aligned} m_B^2 - m_{\pi\pi}^2 &\simeq (m_{h^+}^2 - m_\pi^2) + (m_{h^-}^2 - m_\pi^2) + \\ &+ 2p_+p_- \left[\left(1 + \frac{m_{h^+}^2}{2p_+^2}\right) \cdot \left(1 + \frac{m_{h'^-}^2}{2p_-^2}\right) - \left(1 + \frac{m_\pi^2}{2p_+^2}\right) \cdot \left(1 + \frac{m_\pi^2}{2p_-^2}\right) \right] \simeq \\ &\simeq (m_{h^+}^2 - m_\pi^2)\left(1 + \frac{p_-}{p_+}\right) + (m_{h^-}^2 - m_\pi^2)\left(1 + \frac{p_+}{p_-}\right) = \\ &= (m_{h^+}^2 - m_\pi^2)\left(1 + \frac{1-\beta}{1+\beta}\right) + (m_{h^-}^2 - m_\pi^2)\left(1 + \frac{1+\beta}{1-\beta}\right), \end{aligned} \tag{26}$$

where we have introduced the momentum asymmetry β, defined as:

$$\beta = \frac{p_+ - p_-}{p_+ + p_-}. \tag{27}$$

For a given value of β, the mass distribution under the $\pi^+\pi^-$ hypothesis can then be written as:

$$f(m_{\pi\pi}|\beta) = g\left(m_{\pi\pi}; \sqrt{m_B^2 - F_{h^+h'^-}(\beta)}\right), \tag{28}$$

where $g(m; m_B)$ is the mass p.d.f. for a B meson of true mass m_B, defined using the correct hypothesis for the daughter particles, and the function $F_{h^+h'^-}(\beta)$ is defined as:

$$F_{h^+h'^-}(\beta) = (m_{h^+}^2 - m_\pi^2)\left(1 + \frac{1-\beta}{1+\beta}\right) + (m_{h^-}^2 - m_\pi^2)\left(1 + \frac{1+\beta}{1-\beta}\right). \tag{29}$$

In practice, for a given value of β, the m_B mass is shifted towards lower mass values by an amount equal to $\Delta(\beta) = m_B - \sqrt{m_B^2 - F_{h^+h'^-}(\beta)}$.

It is now straightforward to write the joint p.d.f. for $m_{\pi\pi}$ and β, by multiplying $f(m_{\pi\pi}|\,\beta)$ by a p.d.f. for β:

$$f(m_{\pi\pi},\,\beta) = g\left(m_{\pi\pi};\sqrt{m_B^2 - F_{h^+h'^-}(\beta)}\right)\cdot h(\beta). \tag{30}$$

Fig. 4 shows the distributions of $m_{\pi\pi}$ versus β for offline selected full MC events.

In the case of the $B^0 \to \pi^+\pi^-$ decay, as shown in Fig. 5, we have found empirically that an accurate parameterization for $h(\beta)$ is:

$$h(\beta) = K^{-1}\Theta(|\beta_0| - |\beta'|)\sqrt{1 - \frac{\beta'^2}{\beta_0^2}} \otimes G(\beta - \beta';\sigma_\beta), \tag{31}$$

where K is a normalization factor, β_0 is a free parameter and $G(\beta - \beta';\,\sigma)$ is a Gaussian with width equal to the free parameter σ_β.

Although we expect $h(\beta)$ to be very similar for all the channels, at least as far as the shape is concerned, there is a kinematical constraint induced by the lower limit of the $\pi^+\pi^-$ invariant mass window, that according to the event selection is $m_{min} = 5\,\mathrm{GeV/c^2}$, which visibly modifies $h(\beta)$ when the daughter particles are not pions. In fact, neglecting experimental resolutions, the following inequality holds:

$$\sqrt{m_B^2 - F_{h^+h'^-}(\beta)} > m_{min}, \tag{32}$$

which leads to the allowed range for β

$$\beta_- < \beta < \beta_+, \tag{33}$$

where

$$\beta_\pm = \frac{\Delta m_+^2 - \Delta m_-^2 \pm \sqrt{(\Delta m_+^2 - \Delta m_-^2)^2 - \Delta m_B^2\cdot(2\Delta m_+^2 + 2\Delta m_-^2 - \Delta m_B^2)}}{\Delta m_B^2} \tag{34}$$

with

$$\Delta m_\pm^2 = m_{h^\pm}^2 - m_\pi^2 \tag{35}$$

and

$$\Delta m_B^2 = m_B^2 - m_{min}^2. \tag{36}$$

In practice, the effect of the $\pi^+\pi^-$ invariant mass cut on $h(\beta)$ is to introduce an abrupt cutoff at the β_- and β_+ limits (see Tab. 4 for the actual values of β_- and β_+). Indeed, due to resolution effects, we do not expect the previous inequalities to be strictly valid, but nonetheless to be a good approximation.

In order to obtain a general expression of the p.d.f. for β we can proceed as follows. If $h(\beta)$ and $f(m_{\pi\pi}|\beta)$ are the p.d.f.'s for β and $m_{\pi\pi}$ given the value of β in the absence

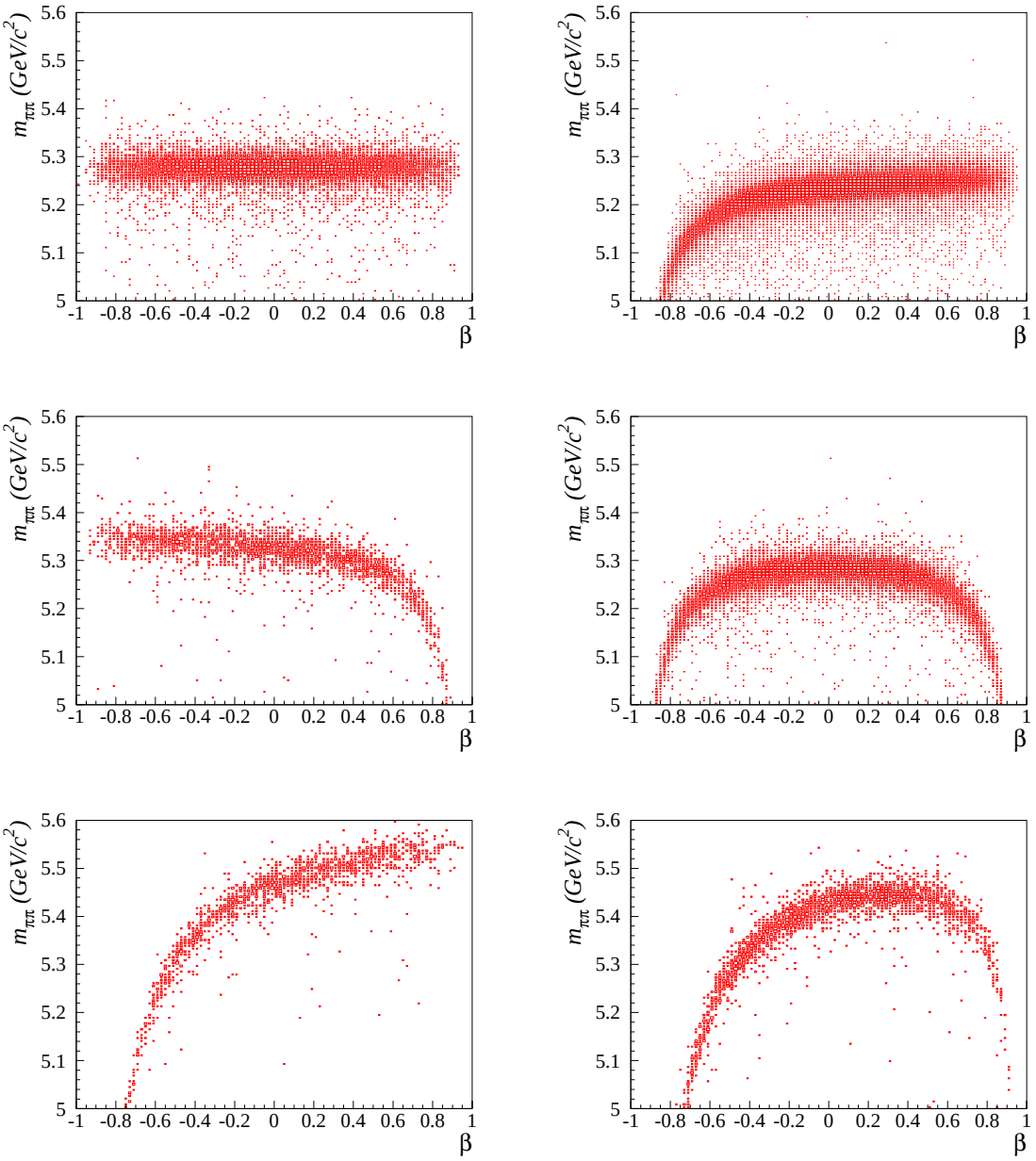

Figure 4: Distributions of the invariant mass $m_{\pi\pi}$ versus the momentum asymmetry β for offline selected events: $B^0 \to \pi^+\pi^-$ (top left), $B^0 \to K^+\pi^-$ (top right), $B_s^0 \to \pi^+K^-$ (middle left), $B_s^0 \to K^+K^-$ (middle right), $\Lambda_b \to p\pi^-$ (bottom left) and $\Lambda_b \to pK^-$ (bottom right). Note that, for the flavour specific decays, β transforms to $-\beta$ when passing from a decay to its $\mathcal{CP}$-conjugate. For this reason, the β values of $\mathcal{CP}$-conjugate decays have been reflected around $\beta = 0$ in order to increase the available statistics.

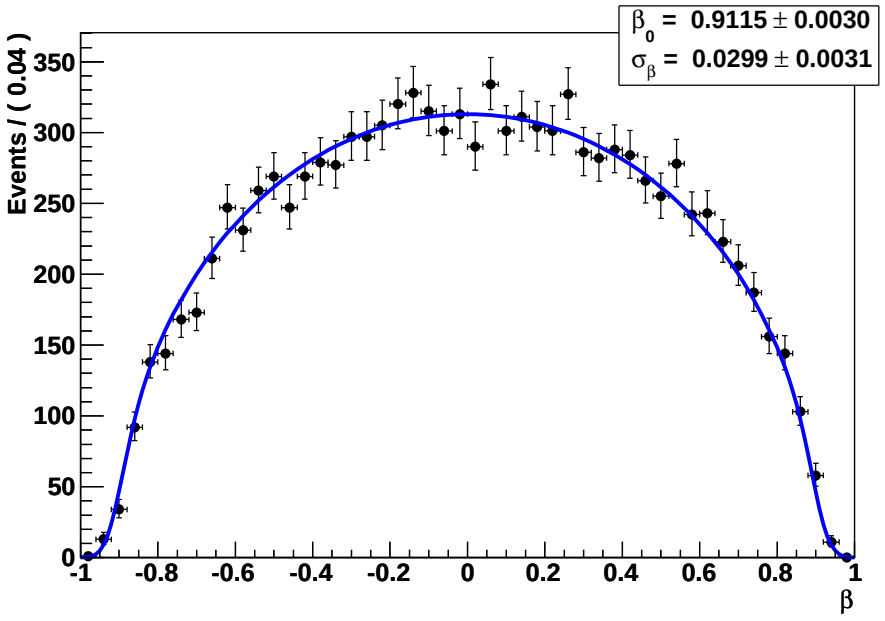

Figure 5: Distribution of the momentum asymmetry β for $B^0 \to \pi^+\pi^-$ offline selected events, with the result of an unbinned likelihood fit of the p.d.f., defined in Eq. (31), superimposed.

of any mass cut, the p.d.f. for $m_{\pi\pi}$ and β, when a mass cut between m_{min} and m_{max} is applied, is given by:

$$\tilde{f}(m_{\pi\pi},\, \beta) = \frac{f(m_{\pi\pi}|\beta)h(\beta)}{\int_{-1}^{1} d\beta' h(\beta') \int_{m_{min}}^{m_{max}} dm'_{\pi\pi} f(m'_{\pi\pi}|\beta')}. \tag{37}$$

The p.d.f. for β in the presence of mass cuts is then obtained by integrating this expression with respect to $m_{\pi\pi}$:

$$\tilde{h}(\beta) = \frac{h(\beta) \int_{m_{min}}^{m_{max}} f(m'_{\pi\pi}|\beta) dm'_{\pi\pi}}{\int_{-1}^{1} d\beta' h(\beta') \int_{m_{min}}^{m_{max}} dm'_{\pi\pi} f(m'_{\pi\pi}|\beta')}. \tag{38}$$

By approximating for simplicity $f(m_{\pi\pi}|\beta)$ as a single Gaussian

$$f(m_{\pi\pi}|\beta) = G(m_{\pi\pi};\, \mu(\beta),\, \sigma), \tag{39}$$

with mean $\mu(\beta) = \sqrt{m_B^2 - F_{h^+h^-}(\beta)}$ and width $\sigma \simeq 25\,\mathrm{MeV/c^2}$, i.e. the average width of the mass distributions under the correct mass hypotheses (see Tab. 3), we obtain:

$$q(\beta) = \int_{m_{min}}^{m_{max}} f(m'_{\pi\pi}|\beta) dm'_{\pi\pi} = \frac{1}{2}\left[\mathrm{Erf}\left(\frac{m_{max} - \mu(\beta)}{\sqrt{2}\sigma}\right) - \mathrm{Erf}\left(\frac{m_{min} - \mu(\beta)}{\sqrt{2}\sigma}\right)\right]. \tag{40}$$

Channel	β_-	β_+
$B^0 \to \pi^+\pi^-$	-1	1
$B^0 \to K^+\pi^-$	-0.844	1
$B_s^0 \to \pi^+K^-$	-1	0.883
$B_s^0 \to K^+K^-$	-0.875	0.875
$\Lambda_b \to p\pi^-$	-0.740	1
$\Lambda_b \to pK^-$	-0.730	0.922

Table 4: Values of the β_- and β_+ parameters, calculated using Eq. (34).

As a consequence, the general expression of the p.d.f. for β becomes:

$$\tilde{h}(\beta) = \frac{h(\beta) \cdot q(\beta)}{\int_{-1}^{1} h(\beta') \cdot q(\beta') d\beta'}, \tag{41}$$

with $h(\beta)$ given by Eq. (31).

Fig. 6 shows the distributions $\tilde{h}(\beta)$ for all the decay modes under study, with the p.d.f. of Eq. (41) superimposed. The values of the parameters β_0 and σ_β have been fixed to the ones determined by fitting the $B^0 \to \pi^+\pi^-$ spectrum (see Fig. 5). As expected, the p.d.f.'s are characterized by abrupt cutoffs at the values of β_- and β_+ reported in Tab. 4.

By employing the parameterization of the invariant mass under the correct mass hypothesis introduced in Eq. (20), we are finally able to write the joint p.d.f. for $m_{\pi\pi}$ and β as follows:

$$\begin{aligned} \tilde{f}(m_{\pi\pi},\, \beta) \;&=\; [f_E\, E_d(m - \mu(\beta);\, f_1,\, \sigma_1,\, \sigma_2,\, s) + \\ &+\; (1 - f_E)\, C\, G_d(m - \mu(\beta);\, f_1,\, \sigma_1,\, \sigma_2)] \cdot \tilde{h}(\beta), \end{aligned} \tag{42}$$

where the factor C normalizes the double Gaussian G_d to 1 inside the mass window.

Fig. 7 shows the invariant mass distributions under the $\pi^+\pi^-$ hypothesis for the various decay modes, with the projections on $m_{\pi\pi}$ of the results of unbinned likelihood fits of the p.d.f. defined in Eq. (42) to the spectra. The numerical results of the fits are summarized in Tab. 5. The fitted curves describe the data well, and the numerical results of Tab. 5 are in very good agreement with those obtained by studying the mass distributions under the correct mass hypothesis, summarized in Tab. 3. It must be emphasized that, although the original MC samples on which the fits are performed are the same, we do not expect the results of Tabs. 3 and 5 to be strictly identical. Besides additional approximations, in the latter case we are imposing that the $m_{\pi\pi}$ mass is inside a given window, while this is not required in the former case, except of course for the $B^0 \to \pi^+\pi^-$ decay, where the $\pi^+\pi^-$ hypothesis is the correct one. The requirement on $m_{\pi\pi}$ leads to a greater probability of discarding events which are placed in the radiative tail of the mass distributions under the correct mass hypothesis. Hence we expect to have reduced sensitivity for the parameters describing the radiative tail, since indeed we have fewer events where large radiation occurred surviving the cut on $m_{\pi\pi}$.

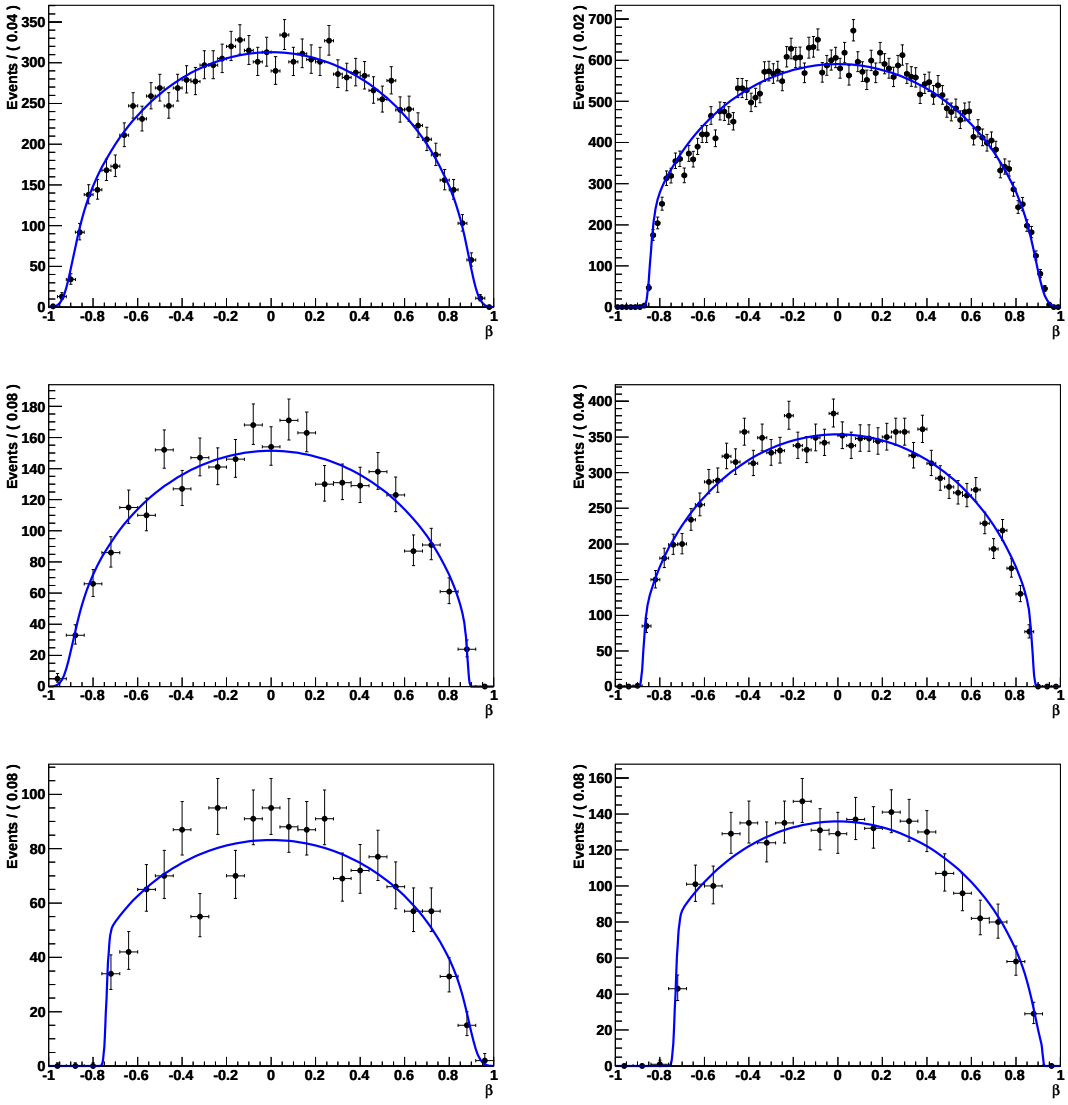

Figure 6: Distributions of the momentum asymmetry β for offline selected events, with the p.d.f. defined in Eq. (41) superimposed: $B^0 \to \pi^+\pi^-$ (top left), $B^0 \to K^+\pi^-$ (top right), $B_s^0 \to \pi^+K^-$ (middle left), $B_s^0 \to K^+K^-$ (middle right), $\Lambda_b \to p\pi^-$ (bottom left) and $\Lambda_b \to pK^-$ (bottom right). Note that, for the flavour specific decays, β transforms to $-\beta$ when passing from a decay to its $\mathcal{CP}$-conjugate. For this reason, the β distributions of $\mathcal{CP}$-conjugate decays have been reflected around $\beta = 0$ and summed up in the same histograms in order to increase the available statistics.

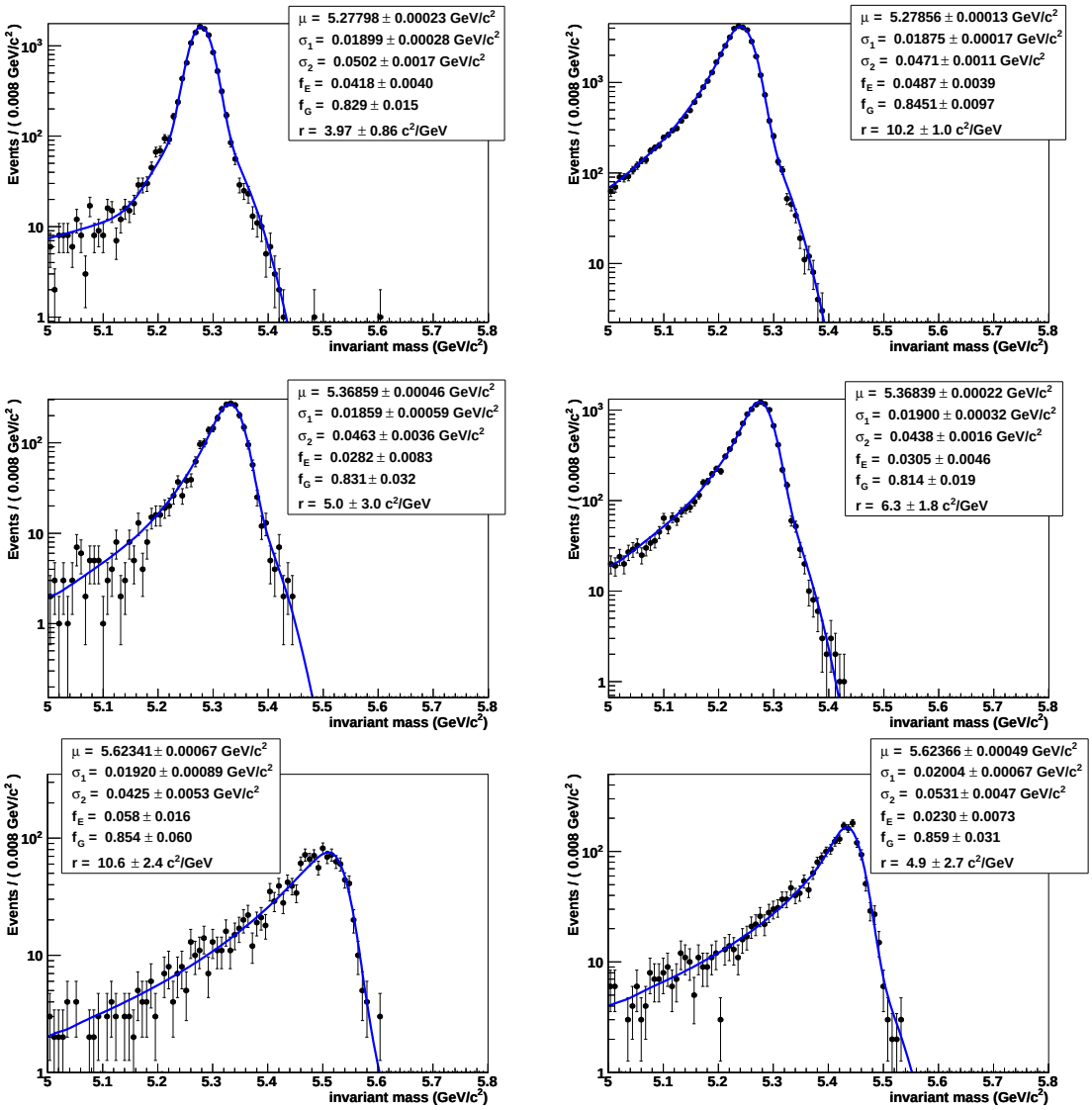

Figure 7: Invariant mass distributions of the various modes under the $\pi^+\pi^-$ hypothesis, with superimposed the projections on $m_{\pi\pi}$ of the results of unbinned likelihood fits of the p.d.f. defined by Eq. (42): $B^0 \to \pi^+\pi^-$ (top left), $B^0 \to K^+\pi^-$ (top right), $B_s^0 \to \pi^+K^-$ (middle left), $B_s^0 \to K^+K^-$ (middle right), $\Lambda_b \to p\pi^-$ (bottom left) and $\Lambda_b \to pK^-$ (bottom right).

Channel	μ [MeV/c^2]	f_G	σ_1 [MeV/c^2]	σ_2 [MeV/c^2]	f_E	r [c^2/GeV]	μ_{MC} [MeV/c^2]
$B^0 \to \pi^+\pi^-$	5278.5 ± 0.3	0.832 ± 0.018	18.8 ± 0.3	47 ± 2	0.066 ± 0.007	9.6 ± 1.2	5279.4
$B^0 \to K^+\pi^-$	5278.6 ± 0.1	0.835 ± 0.010	18.8 ± 0.2	47 ± 1	0.049 ± 0.004	10.2 ± 1.0	5279.4
$B_s^0 \to \pi^+K^-$	5368.6 ± 0.5	0.83 ± 0.03	18.6 ± 0.6	46 ± 4	0.028 ± 0.008	5.0 ± 3.0	5369.6
$B_s^0 \to K^+K^-$	5368.4 ± 0.2	0.814 ± 0.019	19.0 ± 0.3	44 ± 2	0.031 ± 0.005	6.3 ± 1.8	5369.6
$\Lambda_b \to p\pi^-$	5623.4 ± 0.7	0.85 ± 0.06	19.2 ± 0.9	43 ± 5	0.058 ± 0.016	10.6 ± 2.4	5624.0
$\Lambda_b \to pK^-$	5623.7 ± 0.5	0.86 ± 0.03	20.0 ± 0.7	53 ± 5	0.023 ± 0.007	4.9 ± 2.7	5624.0

Table 5: Results of the fits to the distributions ($m_{\pi\pi}$, β) of the p.d.f. defined by Eq. (42). For comparison, the last column shows the mass value used in the MC simulation.

5 Conclusions

We have shown how to describe the line shape of the mass distribution for each $H_b \to h^+h'^-$ decay mode, either using the correct mass hypothesis or, as a conventional choice, the $\pi^+\pi^-$ hypothesis. The description of the invariant mass line shape under a common mass hypothesis is an important ingredient for performing maximum likelihood fits including all the decay modes simultaneously, as discussed in Ref. [2].

Due to the presence of QED final state radiation, each mass distribution presents a long tail on the lower side of the mass peak. The LHCb Monte Carlo simulation makes use of the PHOTOS generator [4] in order to simulate QED radiation in decays, which employs the calculation of $\mathcal{O}(\alpha)$ radiative corrections for charged particles using a leading log collinear approximation. In order to construct a parameterization which takes into account the effect of QED radiation on the invariant mass spectrum, we employed an exact calculation of the differential decay rate as a function of the emitted photon energy, made available in Ref. [6]. Such a calculation was specifically performed for the non-leptonic decays of B and D mesons to two pseudo-scalars.

We have also seen that the effect of QED radiation on the mass distributions can be well described by means of a phenomenological parameterization. Although slightly less accurate with respect to the theoretical one, such a parameterization is much simpler and faster to calculate in a computer program, and can be useful when performing maximum likelihood fits with large data samples, where timing may become an effective limiting factor.

References

[1] A. A. Alves *et al.* [LHCb Collaboration], JINST **3** (2008) S08005.

[2] B. Adeva *et al.* [LHCb Collaboration], LHCb-PUB-2009-029 [arXiv:0912.4179].

[3] P. Nason *et al.*, arXiv:hep-ph/0003142.

[4] P. Golonka and Z. Was, Eur. Phys. J. C **45** (2006) 97 [arXiv:hep-ph/0506026].

[5] D. J. Lange, Nucl. Instrum. Meth. A **462** (2001) 152.

[6] E. Baracchini and G. Isidori, Phys. Lett. B **633** (2006) 309 [arXiv:hep-ph/0508071].